Available online at www.sciencedirect.com
SCIENCE DIRECT®
Catalysis Today 100 (2005) 79–94
CATALYSIS TODAY
www.elsevier.com/locate/cattod

Recent conceptual advances in the catalysis science of mixed metal oxide catalytic materials

Israel E. Wachs*

Operando Molecular Spectroscopy and Catalysis Laboratory, Department of Chemical Engineering, Lehigh University, Bethlehem, PA 18015, USA

Available online 18 January 2005

Abstract

The catalysis science of mixed metal oxides (supported metal oxides, molecular sieves and bulk mixed metal oxides) has undergone dramatic paradigm changes over the past 25 years as new characterization techniques became available (X-ray absorption spectroscopy (EXAFS/XANES/soft XANES), Raman, solid-state NMR, HR-TEM, UV–vis DRS and LEISS) to catalysis researchers. The major advantages offered by these spectroscopic improvements are that (1) they can detect XRD inactive amorphous surface metal oxide phases as well as crystalline nanophases and (2) their ability to collect information under various environmental conditions. Application of these spectroscopic techniques to the investigation of mixed metal oxide catalysts have provided new fundamental insights into the electronic and molecular structures of mixed metal oxide catalytic active sites and how they control the catalytic activity and selectivity characteristics. The most significant discovery has been that amorphous metal oxide phases are always present and are the catalytic active sites for many applications of mixed metal oxide catalysts. This has resulted in a significant paradigm shift as to how mixed metal oxide catalytic materials function for different applications. This article reviews the instrumental advances and the resulting conceptual advances that have evolved over the past 25 years in the catalysis science of mixed metal oxide catalysts.
© 2004 Elsevier B.V. All rights reserved.

Keywords: Catalysts; Metal oxides; Supported; Molecular sieves; Bulk; Vanadium oxide; V_2O_5; Oxidation; CH_3OH; C_3H_8; C_4H_{10}; SO_2; CH_3SH; Thiophene

1. Introduction

The catalysis science of metal-based catalysts, bulk as well as supported, was significantly advanced in the 1970s by (1) introduction of selective chemisorption methods to determine the number of exposed metal sites, (2) transmission electron microscopy (TEM) for imaging the structure and morphology of the metallic components, (3) X-ray diffraction (XRD) for determining the volume average particle dimensions, (4) X-ray absorption spectroscopy (EXAFS/XANES) for determining local coordination, and (5) UHV model single crystal studies [1–5]. This allowed for the successful quantitative comparison of reaction rates between different catalysis laboratories as well as supported metal catalysts and model large single crystals [1–3]. In contrast, the catalysis science of mixed metal oxide catalysts was not sufficiently developed in the 1970s and significantly lagged the rapid advances being achieved in the catalysis science of metal catalysts [6,7]. The major reasons for the much slower development of the catalysis science of mixed metal oxide catalysts are (1) that mixed metal oxide catalysts are significantly more complex than metal-based catalysts (e.g., possible presence of multiple oxidation states, variable local coordination, coexisting bulk and surface phases as well as different surface termination functionalities such as M–OH, M=O, or M–O–M) and (2) the need for the development of new spectroscopic methods that can determine such fundamental electronic and molecular structural details. The objective of this article is to review the growth of mixed metal oxide catalysis science over the past three decades and to assess the current status of this important area of catalysis. Zeolitic materials will not be discussed in this article since by definition their structures are made up from Al and Si TO_4 units that are not metal oxides [8]. Molecular sieves containing transition metal

* Tel.: +1 610 7584274; fax: +1 610 7586555.
E-mail address: iew0@lehigh.edu.

0920-5861/$ – see front matter © 2004 Elsevier B.V. All rights reserved.
doi:10.1016/j.cattod.2004.12.019

oxides (e.g., Ti, V, Nb, etc.), however, will be covered in this article on mixed metal oxides. Another class of emerging mixed metal oxide catalysts is Keggin, Anderson and Dawson clusters, which has recently been reviewed [9,10].

2. Development of spectroscopic instrumentation

2.1. 1950s–1970s

The past three decades has seen a revolution in the development of spectroscopic catalyst characterization techniques and many of these instrumental advances have had significant impacts on the challenging catalysis science of mixed metal oxide catalytic materials. These spectroscopic instruments serve are our ''eyes'' into the sub-nanometer molecular world of catalytic metal oxide surfaces and their novel surface chemistry with different molecules. Consequently, not surprisingly, many of the recent advances in catalysis science have paralleled the development of new spectroscopic instrumentation during this rapidly expanding period. There were several events prior to the past three decades that set the stage for the advances that occurred in this time period. Mapes and Eischens reported the first successful demonstration of in situ infrared (IR) spectroscopic measurements of chemisorbed molecules on catalytic metals and zeolites in 1954 [11]. These groundbreaking studies showed that with IR spectroscopy it was possible to discriminate between surface Lewis and Bronsted acids by chemisorption of NH_3 and measure the vibrational spectrum of $NH_{3(ads)}$ and $NH_{4(ads)}^{+}$, respectively. Lunsford and Kazasky were among the first catalysis researchers that were active in the 1960s in developing electron proton resonance (EPR) techniques for characterization of catalytic materials and surface intermediates [12]. It was shown by these and other researchers that were active in this area at the time that EPR can provide information about the presence and local coordination of paramagnetic species (e.g., Mo^{+5}, V^{+4}, Cr^{+5}, Cr^{+3}, etc.). Siegbahn also developed X-ray photoelectron spectroscopy (XPS) in the late 1950s and 1960s that allows determination of the surface region of catalytic materials [13]. These exciting developments in XPS led to the introduction of commercial XPS units in the 1970s [14]. Solid-state magic angle spinning-nuclear magnetic resonance (MAS-NMR) and intense monochromatic lasers were just being developed in the late 1960s. However, the discovery of XRD at the beginning of the 20th century to determine long range order of crystalline phases dominated the available catalyst characterization arsenal due to its sound scientific development over the century. This was the status of the spectroscopic characterization methods available to catalysis researchers ~30 years ago.

These spectroscopic capabilities, however, were not developed enough to significantly advance the catalysis science of catalytic mixed metal oxide materials with the exception of XRD. Although IR provided information about chemisorbed molecules on oxide surfaces, it was not able to provide fundamental molecular structural information about the metal oxide catalytic active sites on surfaces because such vibrations are typically obscured by the strong bulk or oxide support vibrations in the region of interest, usually appearing below 1000 cm^{-1}, and many of the chemical probe molecules developed for metals only adsorbed with extreme difficulty on metal oxide surfaces (e.g., O_2, H_2, CO, etc.). The full potential of XPS was not fully tapped at that moment and EPR spectroscopy is only able to provide information about paramagnetic species that only represent a very small fraction, ~1/100, of the total catalytic sites. Furthermore, the small signals detected with EPR may not even be kinetically relevant in many cases or associated with the presence of impurities. It should also be noted that the escape depth of conventional XPS is typically ~3–5 nm, which means that many layers of the mixed metal oxide material are simultaneously being sampled by this spectroscopic technique and the surface component of the signal becomes diluted by the signal from the underlying layers. Thus, catalysis scientists were not equipped at that point in time to fundamentally address the molecular nature of the catalytic active sites, especially surface sites that do not possess long range order, present in mixed metal oxide catalysts and the influence of different environments on their electronic and molecular structures.

2.2. 1970s–1990s

This situation began to rapidly change during the 1970s and 1980s as several new electronic and molecular structural characterization techniques became available and were further advanced (intense monochromatic laser sources and faster detectors for Raman spectroscopy, high energy synchrotron X-ray sources for X-ray absorption spectroscopy (XAS), stronger magnetic fields for solid-state nuclear magnetic resonance (NMR)) and commercial instruments to measure UV–vis diffuse reflectance spectroscopy (DRS) spectra. In contrast to XRD that requires long range order for signal detection, these spectroscopic techniques do not require long range order for signal detection and provide local electronic and molecular structural information. Although these characterization techniques are bulk techniques that sample the entire sample volume rather than the surface, they are able to also yield surface information when the catalytic active component is highly dispersed (molecular sieves and supported metal oxides) in the catalyst sample. For example, the active metal oxide component is typically 100% dispersed throughout the sample volume in molecular sieves, either in framework or as extra-framework sites [8], and on the surface of supported metal oxide catalysts [7]. Recent advances, to be discussed below, have further extended these bulk characterization techniques to also provide surface information about bulk mixed metal oxide catalytic materials.

It cannot be overemphasized, even in the beginning of the 21st century, that heterogeneous catalysis is a surface

phenomenon between molecules and exposed catalytic active sites, rather than sites imbedded within bulk structures. Consequently, fundamental knowledge about the catalytic events at exposed catalytic active sites, on solid surfaces in contact with either gas or liquid phases, is critical to understanding catalytic events. It is, however, also important to determine if the nature of the surface catalytic active sites is also being influenced by the underlying bulk oxide material. In all cases, fundamental catalytic surface electronic and molecular structural information is of paramount importance for understanding and advancing catalysis science.

2.3. Raman spectroscopy

Advances in Raman spectroscopy, intense monochromatic laser excitation sources with improved monochromators and detectors, allowed for the first time, to be confirmed a few years later by Chan et al. [15], the detection of surface metal oxide species for supported MoO_3 [16], WO_3 [17], V_2O_5 [18,19], and Re_2O_7 [20] catalysts during the latter part of the 1970s. This was rapidly followed by reports of in situ Raman studies in the early 1980s where the environment of metal oxide catalytic materials could be controlled (gas phase composition, pressure and temperature) [15,21–24]. The pioneering in situ Raman publication of Chan et al. in 1984 [15] conclusively demonstrated that surface metal oxide species are indeed being detected since they are reversibly changing their structures when exposed to hydrated and dehydrated conditions.

2.4. X-ray absorption spectroscopy

The theory of XAS was in a state of confusion from 1920 to 1970 [25]. The groundbreaking theoretical paper by Sayers et al. [26] changed everything showing that the Fourier transform of the EXAFS with respect to the photoelectron wave number should peak at distances corresponding to nearest neighbor coordination shells of atoms. The accessibility of more intense X-rays at synchrotron radiation sources, three or more orders of magnitude, was greatly enhanced several years after the potential of EXAFS was first shown [27]. The development of synchrotron-based X-ray absorption spectroscopic (XAS) techniques, such as XANES and EXAFS, to characterize catalytic materials followed these early developments. The emphasis of the early studies, however, was on supported metal catalysts and not on metal oxide catalytic materials [26]. Several XANES and EXAFS publications began to appear in the catalysis literature for metal oxide catalytic materials during the mid-1980s and early 1990s (see discussion on supported metal oxide catalysts). XANES provides local coordination symmetry and oxidation states of metal oxides and EXAFS provides more detailed local structural information (M–O bond lengths and coordination sphere of the cations). These structural details nicely complement the Raman and IR vibrational spectroscopic structural information already available at the time and allowed for surface metal oxide molecular structural assignments.

The past few years have again seen significant advances in XAS with the development of soft X-ray absorption spectroscopy [28–30]. Soft XAS allows tuning of the electron kinetic energy and the corresponding sampling depth down to ~0.5 nm, which is a dramatic improvement of the 3–5 nm escape depth of conventional XPS instrumentation. In fact, the information from different sample depths can be changed by changing the photon energy. Similar to XPS, soft XAS provides electronic structural information, however, pressures of several Torr are only feasible and allow measurement under very mild reaction conditions. The unique surface sensitivity, variable sample depth analysis and in situ capability at mild pressures of soft XAS assures that this new catalyst characterization technique will be vigorously developed and make significant contributions in the coming years.

2.5. Solid-state NMR

Solid-state nuclear magnetic resonance (NMR) was also being developed during the 1980s, and still continues to be advanced with new methodologies, as a catalyst structural characterization technique to provide local structural details about cations in metal oxide catalytic systems and more recently the surface reaction intermediates [31]. Solid-state NMR can only detect nuclei that are diamagnetic and the presence of paramagnetic cations (Fe^{+3}, Mo^{+5}, Cr^{+5}, Mo^{+5}, W^{+5}, V^{+4}, Cr^{+3}, etc.) interferes with the measurement of NMR signals from diamagnetic cations (^{7}Li, ^{11}B, ^{23}Na, ^{27}Al, ^{29}Si, ^{31}P, ^{51}V, ^{67}Zn, ^{71}Ga, ^{95}Mo, ^{133}Cs, as well as ^{1}H, ^{13}C, ^{15}N and ^{17}O). Most of the emphasis of solid-state NMR during this period was on zeolitic materials because of the intense activity in this area of oxide catalysis [8]. However, throughout the 1980s and 1990s the application of solid-state NMR characterization was continuously being expanded. Solid-state ^{51}V measurements were first reported for bulk mixed metal vanadates by the Russian Boreskov Institute group [32–34] and first reported by Eckert and Wachs [35,36] for supported vanadium oxide catalysts under in situ conditions. During the 1990s, solid-state NMR studies were further expanded to other NMR active nuclei of supported metal oxide catalysts ^{31}P [37], ^{95}Mo [38], ^{29}Si [39], molecular sieves [40] and bulk mixed metal oxides [41,42].

2.6. UV–vis DRS

UV–vis diffuse reflectance spectroscopy (DRS) was also being discovered by catalysis researchers in the 1970s and several early reviews appear in the literature [43–45]. It was not until the 1980s and mid-1990s, however, that UV–vis DRS of metal oxides started to be intensively developed by catalysis researchers involved with metal oxide catalytic

materials [46,47]. Che and co-workers demonstrated that the UV–vis absorption spectrum of MoO_x species changes with the number of Mo species in an oxide cluster [48]. Weber extended these findings to quantitatively determine the Mo oxide cluster band gap, Eg, and demonstrated that it correlates inversely with the number of bridging Mo–O–Mo bonds of the Mo cations [49]. In addition, UV–vis can also monitor the extent of reduction of fully oxidized cations due to ligand to metal charge transfer (LMCT) and the appearance of reduced cations arising from d–d transitions [50]. It was not until the mid-1990s, however, that UV–vis DRS spectra of metal oxide could be quantitatively analyzed within a theoretical framework.

2.7. High resolution-transmission electron microscopy

Significant advances in high resolution-transmission electron microscopy (HR-TEM) were also occurring during this period and provided atomic resolution images of catalytic active sites under controlled environments (<10 torr) [51,52] Most recently, Hansen and co-workers were further expanding such studies to a wide range of catalytic materials and reaction conditions [53–55]. Most of the HR-TEM studies focused on supported metal catalysts and supported metal sulfide catalysts because of the strong contrast between the metallic component and the oxide support [56]. Several attempts were made in the early 1990s to image the two-dimensional surface metal oxide species present in supported metal oxide catalysts, but the lack of long range order in the surface metal oxide monolayers, and the lack of contrast between the surface metal oxide phase and the underlying oxide support has still not allowed for the imaging of the amorphous surface metal oxide monolayers. Furthermore, it was discovered with HR-TEM in 1995 that the surface of the bulk V–P–O catalyst possesses an amorphous skin [57], and more recent HR-TEM studies have revealed that similar situations also take place on the surface of other bulk mixed metal oxide catalysts [58].

2.8. Chemical probe molecules and reactions

''Smart'' chemical probe molecules should be able to (1) quantitatively determine the number of exposed catalytic active sites, (2) discriminate among the different type of surface catalytic active sites (redox, acidic and basic), and (3) provide quantitative information about the relative reaction rates on the different type of surface catalytic sites. Furthermore, it is also important to be able to (4) discriminate between the surface Lewis and Bronsted sites and (5) rank the strength or catalytic rates of the different acidic and basic sites. Although one universal ''smart'' chemical probe molecule does not exist, the desired information can usually be obtained by the use of at least two chemical probe molecules. For example, methanol oxidation over oxide surfaces primarily forms H_2CO over the surface redox sites, dimethyl ether (DME, CH_3OCH_3) over surface acidic sites and primarily CO_x and some H_2CO over surface basic sites. Furthermore, methyl formate (MF, CH_3OOCH) forms on adjacent surface redox–basic sites and dimethoxy methane (DMM, $(CH_3O)_2CH_2$) on adjacent surface redox–acidic sites. Additional surface chemical details can be obtained by basic chemical probe molecules that discriminate between surface Lewis and Bronsted acid sites as well as their corresponding surface basic sites. The CH_3OH chemical probe molecule, however, appears to be emerging as the ''smart'' chemical probe molecule for metal oxide surfaces since it can readily provide information about items 1–3 [59].

2.9. Summary

The tremendous advances in spectroscopic characterization instrumentation and data analysis over the past three decades have allowed catalysis researchers to monitor many more fundamental catalytic details that have led to new concepts, as well as to question old concepts, for catalysis of mixed metal oxides. The discussion below will emphasize the surface electronic and structural aspects of different mixed metal oxide catalytic systems. The one component metal oxide phases, supported metal oxides, and molecular sieves and bulk mixed metal oxide systems will only be discussed because of the author's active involvement in these catalysis research areas during this dynamic period in catalysis science development of mixed metal oxide catalytic materials. Consequently, many of the selected examples will come from the author's own research experience with mixed metal oxide catalysts over the past 25 years (1979–2004).

3. One component metal oxide phases

It is important to initially discuss one component metal oxide phases before addressing the more complex mixed metal oxide catalytic materials. One component metal oxides can crystallize with different morphologies (isotropic, anisotropic or remain amorphous) and local coordination. All one component metal oxide phases will crystallize at elevated temperatures (provide XRD detectable crystalline phases), but many phases may remain amorphous at modest calcination temperatures (e,g., SiO_2, Al_2O_3, Nb_2O_5, Ta_2O_5, etc.). The majority of one component metal oxides crystallize with an isotropic morphology (without preferential orientation) [60], and surface terminate with M–OH, M–O–M, M=O or M-[ ] functionalities where M-[ ] represents an oxygen vacancy [61–64].

Bulk crystalline structures are usually determined with XRD and the surface functionalities are typically determined with vibrational spectroscopic methods such as IR and more recently also by Raman. For example, amorphous isotropic SiO_2 terminates with isolated Si–OH, hydroxyl pairs of $(Si–OH)_2$ and $Si(–OH)_2$, and bridging Si–O–Si

bonds [65] and isotropic Nb_2O_5, crystalline as well as amorphous, terminates with Nb–OH, Nb–O–Nb and Nb=O bonds [61]. In the case of crystalline isotropic Cr_2O_3, both surface Cr^{+3} and Cr^{+6} oxidation states are present and the surface terminates with Cr–OH, Cr–O–Cr and Cr=O functionalities [63]. Surfaces that terminate with M=O bonds typically possess M^{+7}, M^{+6} and M^{+5} cations, and surfaces with M^{+4}, M^{+3}, M^{+2} and M^{+1} cations typically do not possess enough electrons to form terminal M=O bonds and terminate with M–OH or M–O–M bonds. Furthermore, most low valent oxides typically only exhibit surface Lewis acidity and most high valent oxides typically contain both surface Lewis and Bronsted acidity [66,67].

It is important to emphasize that these various surface functionalities usually possess different surface reactivity properties. For example, when metal oxides and molecules are adsorbed on the SiO_2 surface the anchoring sites are the more reactive isolated surface Si–OH groups and not the less reactive bridging Si–O–Si and adjacent hydrogen bonded surface hydroxls [68]. In the case of Al_2O_3, multiple surface hydroxyls are present as well as oxygen vacancies or defects [69,70]. The different surface hydroxyls vary by the number of Al sites and Al coordination, which determine their surface chemistry characteristics [65]. The isolated Al–OH sites are the most basic and the bridging Al–OH–Al sites are the most acidic. As for SiO_2, the isolated Al–OH sites are the most reactive when metal oxides or molecules are adsorbed on the alumina surface. The Al-[ ] surface defects possess Lewis acidity character [71]. Furthermore, the Cr^{+6} terminal Cr=O bonds on the surface of crystalline Cr_2O_3 undergo redox processes in reactive environments because of the ability of such sites to readily become reduced to lower oxidation states and lose their O atoms to reducing reactants.

Some metal oxides crystallize with an anisotropic morphology such as platelets [60,64]. For example, both crystalline MoO_3 and V_2O_5 crystallize with the platelet morphology where the terminal M=O and bridging M–O–M functionalities are present on the basal planes, and the terminal M–OH predominates on the edge plains [64,72]. Sleight and co-workers nicely demonstrated that the MoO_3 basal plane containing the terminal Mo=O and bridging Mo–O–Mo bonds do not chemisorb CH_3OH and that the surface Mo–OH sites on the edges react with CH_3OH to form surface Mo–OCH_3 and H_2O [73]. The same platelet morphology and relative activity pattern was also found for crystalline V_2O_5 and ZnO when exposed to CH_3OH [74–76].

For platelet morphology, consequently, the number of catalytic active sites of such materials tends to only be a small fraction of the total surface metal oxide sites. These findings reflect the structure sensitivity of metal oxide active sites to different crystalline planes, and the specific surface functionalities present on the different planes. For example, the surface M=O functionality present in crystalline MoO_3 and V_2O_5 is catalytically relatively inactive relative to the surface M–OH functionality in these catalysts. Theoretical calculations on crystalline V_2O_5 have also confirmed that the surface M=O functionality is too stable relative to other surface functionalities for catalytic reactions [77].

As can be concluded from the above discussion, catalytic metal oxides are much more complex than the corresponding metal-based catalysts because they can terminate with multiple surface functionalities and exhibit several cation oxidation states.

4. Supported metal oxide systems

4.1. Surface metal oxide phases

Supported metal oxide catalysts are created when an active metal oxide component is deposited on an oxide support [7]. The active acidic metal oxides (e.g., ReO_x, CrO_x, MoO_x, WO_x, VO_x, NbO_x, TaO_x, etc.) usually anchor to the oxide substrate by preferentially titrating the basic surface hydroxls of oxide supports [78]. The active basic metal oxides (FeO_x, NiO_x, CoO_x, etc.), however, usually anchor to the oxide substrate by preferentially titrating the surface Lewis acid sites, such as surface M-[ ] vacancies, of the oxide support [79]. For many supported metal oxide systems, the active component is usually present as a ~100% dispersed surface metal oxide phase (typically when Al_2O_3, TiO_2, ZrO_2, Nb_2O_5 and Ta_2O_5 are used as the oxide supports) below monolayer surface coverage. Less than 100% dispersion is usually obtained for metal oxides on the SiO_2 support because of the lower reactivity and more acidic character of its surface hydroxyls [80]. In addition, some active basic metal oxide components do not interact strongly with the different oxide functionalities present on oxide supports and, consequently, do not disperse very well to form nanocrystalline phases (e.g., MnO_x, CeO_x, etc.) [81]. The electronic and molecular structures of the surface metal oxide species that are present on oxide supports have received enormous attention over the past three decades because of (1) their industrial significance as catalysts for numerous applications [82] and (2) their ability to serve as model mixed metal oxide catalytic system due to the essentially completely dispersed state.

4.2. Molecular structures of dehydrated surface vanadium oxide species

The supported vanadium oxide catalytic systems have probably received the most attention in the catalysis literature during this period because of intense interest in their multiple industrial applications and will be the focus of this section for brevity. The surface nature of the supported VO_x catalysts was clearly revealed by the application of several ground breaking in situ spectroscopic investigations during the 1980s: Raman [15], XANES/EXAFS [83], solid-state ^{51}V NMR [35,36] and IR [84]. Both the solid-state ^{51}V NMR and the XANES/EXAFS measurements revealed VO_4

coordination for the dehydrated surface VO_x species. The coincidence of the Raman and IR bands from the terminal V=O bond could only occur if only one terminal bond was present for the dehydrated surface VO_x species, and was further confirmed by $^{18}O_2$–$^{16}O_2$ studies as well as IR studies in the overtone region [72]. The presence of bridging V–O–V bonds was readily detected with Raman [85] and the polymeric nature of the dehydrated surface species were confirmed by complementary UV–vis measurements [86]. The dehydrated surface VO_x species are usually exclusively present as isolated surface $O{=}V(O{-}S)_3$ species at low surface coverage and the extent of polymerization increases with surface VO_x coverage that can reach as much as ~100% polymerized species at monolayer surface coverage [87]. Above monolayer surface coverage, crystalline V_2O_5 nanoparticles form on top of the surface vanadia monolayer because all the exposed and reactive support surface hydroxyls have been consumed in anchoring the two-dimensional surface vanadia phase [78]. The local coordination present in bulk V_2O_5 is made of a polymeric VO_5 unit with mono–oxo terminal V=O bond [60]. The platelet morphology and inactive basal planes of crystalline V_2O_5 result in very few new catalytic active sites and actually tend to decrease the number of exposed surface VO_x by covering them. Thus, the spectroscopic studies revealed that there are three distinct dehydrated surface vanadia sites on supported vanadia catalysts as a function of surface coverage: isolated VO_4, polymeric VO_4 and V_2O_5 nanocrystals (see Fig. 1).

4.3. Surface chemistry of supported vanadium oxide species

The surface chemistry of the different supported vanadia species were chemically probed by CH_3OH oxidation to H_2CO [88,89]. The catalytic results were quantified per surface vanadia species as turnover frequencies (TOF = - number of H_2CO molecules formed/surface V/s) because the surface vanadia species were 100% dispersed (confirmed with Raman). The methanol oxidation catalytic results showed that the surface vanadia species exclusively behaved as redox sites since they yielded redox products. Furthermore, the catalytic contribution of the nanocrystalline V_2O_5 phase was minimal primarily because of the low number of active surface edge sites present and that the overall catalytic performance was dominated by the surface vanadia phase. The TOF values for the isolated and polymeric surface VO_4 species, however, were essentially identical since the TOF value did not change with surface vanadia coverage and showed that only one surface VO_4 unit was required for the reaction. In subsequent years, this was also shown to be the case for oxidation reactions requiring only one O atom or two electrons: SO_2 oxidation to SO_3 [90], C_2H_6 oxidation to C_2H_4 [91] and C_3H_8 oxidation to C_3H_6 [90,92,93] as shown in Fig. 2 below. Oxidation reactions requiring more than one O atom or two

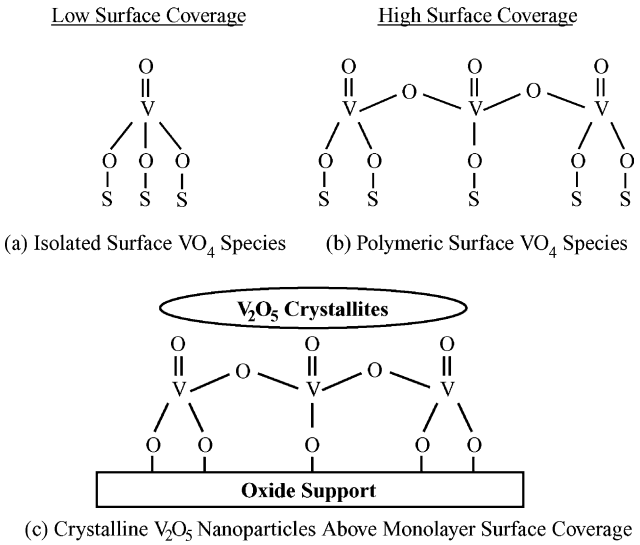

Fig. 1. Supported vanadium oxide catalysts consist of (a) isolated, (b) polymeric surface mono-oxo VO_4 species and (c) crystalline V_2O_5 nanoparticles.

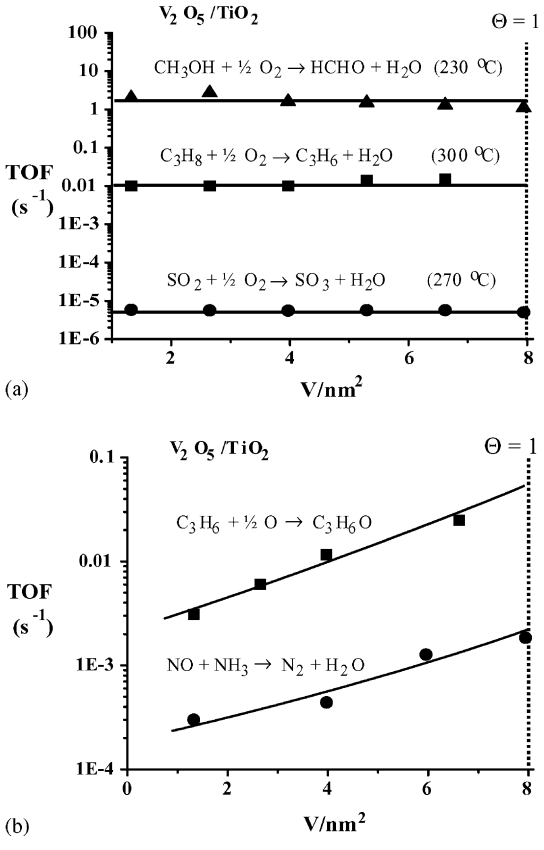

Fig. 2. (a) Isolated and polymeric surface mono-oxo VO_4 species present at low and high surface coverage, respectively, exhibit the same specific catalytic activity, TOF, for two electron reactions that involve one O atom. (b) Oxidation reactions requiring more than one O atom or two electrons, or multiple surface VO_4 sites, exhibit increasing specific catalytic activity, TOF, with surface coverage.

electrons, however, require multiple surface VO_4 sites and the TOF increases with increasing surface VO_4 coverage as shown below: NH_3 SCR of NO to N_2 [94], *n*-butane oxidation to maleic anhydride [95], and C_3H_6 oxidation to acrolein [96].

4.4. Oxidation states of surface vanadium oxide species

In situ Raman and UV–vis measurements during these oxidation reactions revealed that the surface VO_4 species are almost entirely present in the oxidized V^{+5} state during these differing reaction conditions and, consequently, only trace amounts of reduced surface V^{+4}/V^{+3} species are present [92,97]. The relative catalytic contributions of the different surface vanadia oxidation states for methanol oxidation to formaldehyde were examined by Vohs and co-workers [98–101]. By controlling the extent of reduction of the surface phase, the following trend was observed: $V^{+5} > V^{+4} \gg V^{+3}$. Thus, the catalytic active site is the fully oxidized surface VO_4 sites and not the reduced surface vanadia sites. This conclusion is contrary to what has repeatedly been proposed in the catalysis literature by many researchers over the years.

4.5. Reaction kinetics and mechanism

Most of the oxidation reactions over the supported vanadia species occur via a Mars-van Krevelen mechanism, where the participating oxygen comes from the catalyst, the surface vanadia species in this case, and not from gas phase molecular O_2 (Langmuir–Hinshelwood mechanism) [102]. In other words, the only kinetic function of gas phase molecular O_2 is to rapidly oxidize the reduced surface V^{+4} and V^{+3} sites back to V^{+5}. This was demonstrated for CH_3OH oxidation to H_2CO, requiring only one oxygen atom to proceed, by performing CH_3OH-temperature programmed surface reaction (TPSR) spectroscopy experiments where identical results were obtained both in the presence and absence of gas phase O_2 [103]. This was also shown to occur for oxidation of CH_3SH to H_2CO and SO_2 that requires three surface oxygen atoms to proceed [103]. When the experiments were extended to the more demanding oxidation reaction of thiophene oxidation to maleic anhydride and SO_2, requiring six oxygen atoms, the maleic anhydride was not formed in the absence of gas phase molecular O_2 [104]. This reveals that thiophene oxidation to maleic anhydride requires more oxygen than can be provided by the surface vanadia monolayer and that additional gas phase O_2 is also required to complete this demanding oxidation reaction. Thus, thiophene oxidation to maleic anhydride and SO_2 proceeds by a combined Mars–van Krevelen and Langmuir–Hinshelwood mechanism because of the high oxygen requirement for this reaction to proceed over the surface vanadia monolayer. Although Mars and van Krevelen originally only applied their kinetics to oxidation reactions over bulk metal oxide catalysts supplying bulk lattice oxygen, the current studies with supported vanadium oxide catalysts demonstrate that a *surface* Mars–van Krevelen mechanism can also operates for supported redox metal oxide catalysts supplying oxygen from surface metal oxide species.

4.6. Catalytic active oxygen species

The catalytically active surface VO_4 species possess three different functionalities (terminal V=O, bridging V–O–V and bridging V–O-support bonds) and their relative catalytic contributions for oxidation reactions were examined for methanol oxidation [89]. The bridging V–O–V bonds are not kinetically critical since the catalytic TOF value does not increase with increasing surface coverage. In addition, in situ UV–vis DRS measurements reveal that there is a slight preference for reduction of the polymeric surface VO_4 species over the isolated surface VO_4 species during steady-state oxidation reaction conditions [92]. Although the terminal V=O bond of the dehydrated surface vanadia species slightly shifted to higher wavenumbers with increasing surface coverage due to lateral interactions and polymerization, the corresponding catalytic TOF values were essentially identical. Thus, the invariance of the TOF value with surface vanadia coverage shows that the bridging V–O–V bonds and the terminal V=O bonds are not involved in the kinetically relevant rate-determing-step, and implicates the bridging V–O-support bond as the catalytic active site. This observation is a general one since similar trends are also observed for numerous oxidation reactions over supported vanadium oxide catalysts: C_2H_6 oxidation to C_2H_4 [91], C_3H_8 oxidation to C_3H_6 [92,93], SO_2 oxidation to SO_3 [90]. This conclusion is contrary to what has been repeatedly proposed in the catalysis literature for the past three decades and is consistent with the inactivity of the crystalline V_2O_5 basal plane for methanol oxidation that contains both the terminal V=O and bridging V–O–V bonds [74,75].

The contribution of the bridging V–O-support bond to methanol oxidation was examined by varying the specific oxide support for the surface vanadia phase [89]. Essentially, the same isolated and polymeric surface VO_4 species were present on the different oxide supports, with the exception of SiO_2 that only contained isolated surface VO_4 species due to the low surface vanadia coverage achievable on this surface [105]. It was found that the steady-state catalytic TOF value increased by a factor of $\sim 10^3$ as the oxide support was varied: $SiO_2 \ll Al_2O_3 \ll Nb_2O_5/Ta_2O_5 < TiO_2 < ZrO_2 < CeO_2$. This trend was found to inversely correlate with the electronegativity of the different support cations: higher TOF values corresponded to lower support cation electronegativity. This dramatic trend suggests that a lower electronegativity of the support cation results in a higher electron density on the bridging V–O-support bond, which enhances the specific rate of the redox cycle of this catalytic active site (Fig. 3) [106].

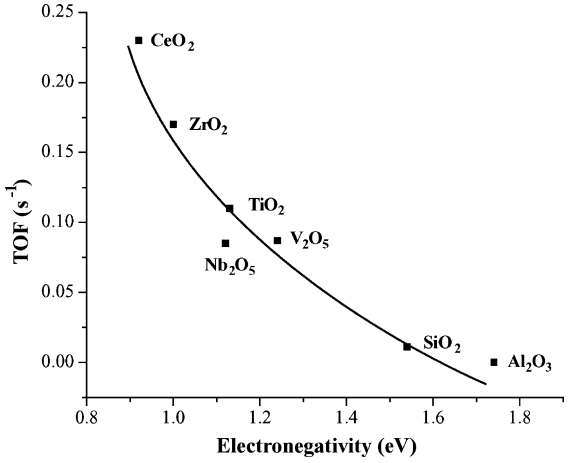

Fig. 3. The catalytic activity per surface vanadia site varies inversely with the support cation electronegativity.

4.7. Influence of the oxide support structure

It is of great fundamental and applied interest to determine if the specific oxide support phase affects the molecular structure and catalytic performance of surface vanadia species. To investigate this important issue, supported vanadia catalysts were synthesized on different TiO_2 phases: rutile, anatase, brookite and B [107]. The TiO_2 supports were laboratory synthesized and their surfaces were analyzed with XPS to confirm that their surfaces were free of any significant impurities. Both Raman and solid-state ^{51}V NMR characterization studies revealed that the same dehydrated surface VO_4 species are present on the different titania support structures, which were synthesized by an identical method (incipient wetness impregnation of a V-triisopropoxide/isopropanol solution in an N_2 environment, dried in an N_2 environment at RT overnight, dried in an N_2 environment at 100 °C overnight, calcined in N_2 at 350 °C and subsequently calcined in air at 450 °C for 2 h). The catalytic properties were chemically probed by the redox methanol oxidation reaction and the TOF values for the different TiO_2 supported vanadia catalysts were essentially invariant and not dependent on the specific titania structure.

The above findings are in contrast to many claims in the catalysis literature over the past 30 years that specific oxide support structures impart enhanced catalytic properties to the catalytic active surface vanadia sites. The reason for this confusion is that commercial oxide supports are synthesized by different processes, which might introduce different surface oxide additives. For example, TiO_2(anatase) is produced by a low temperature sulfate process and its surface is subsequently covered with significant amounts of surface KO_x and PO_x species to retard its photocatalysis activity when applied as a pigment [108]. TiO_2(rutile) is produced by a high temperature process involving the combustion of $TiCl_4$ and ~1% $AlCl_3$ is added to accelerate the anatase to rutile transformation kinetics. The solubility of AlO_x in the TiO_2(rutile) lattice, however, is only ~1/2% and the residual AlO_x segregates to the surface of TiO_2(rutile) particle. Thus, pigment grade commercial TiO_2(anatase) and TiO_2(rutile) possess very different compositions and surface properties. This is the origin for the many contradictory claims in the catalysis literature over the years with regard to the unique characteristics of a specific oxide support phase.

4.8. Influence of the oxide support dimension

The effect of the oxide support size upon the molecular structure of the surface VO_4 species and its catalytic performance was examined for the supported V_2O_5/TiO_2(anatase) system [109]. The standard TiO_2(anatase) support material possessed ~30 nm particles, ~55 m^2/g, and the small TiO_2(anatase) nanoparticles were synthesized in an inert silica matrix to retard the growth of the titania phase during calcination. HR-TEM analysis showed that the dimension of the resulting TiO_2(anatase) nanoparticles varied between 2 and 8 nm as a function of the titania content for the TiO_2/SiO_2 materials. The electronic structure, the band gap (Eg), of the different sized TiO_2(anatase) particles were determined with UV–vis DRS measurements that showed that the TiO_2(anatase) band gap was slightly enhanced for the smallest TiO_2(anatase) nanoparticles [110]. These different sized TiO_2(anatase) supports were subsequently impregnated with a vanadia precursor to synthesize the supported V_2O_5/TiO_2(anatase) catalysts [109]. The inert nature of the SiO_2 support assured that all the vanadia was coordinated to the more active TiO_2(anatase) surfaces. This was confirmed by in situ Raman measurements of the final calcined supported V_2O_5/TiO_2(anatase) catalysts that revealed that the vanadia component was 100% dispersed, no crystalline V_2O_5 present, and that the surface VO_4 species were indeed exclusively coordinated to the TiO_2(anatase) nanoparticles in the TiO_2/SiO_2 catalyst system. The Raman band for the surface vanadia on TiO_2 occurs ~1031 cm^{-1} and that for surface vanadia on SiO_2 is found at ~1041 cm^{-1}, and typical resolution is ~1–2 cm^{-1}. The relatively constant Raman band at ~1031 cm^{-1} revealed that the surface VO_4 species possessed the same molecular structure on the different TiO_2(anatase) particles and was independent of particle size. For the 1% $V_2O_5/TiO_2/SiO_2$ catalyst samples, the surface VO_4 species are essentially present as isolated species. The catalytic TOF values of the isolated surface VO_4 species on the different sized TiO_2(anatase) particles were found to slightly decrease with decreasing TiO_2(anatase) particle size. There may have also been a minor contribution to the TOF values for the larger TiO_2 particles from some heat transfer limitations since the amount of inert SiO_2 deceased in the samples as the TiO_2 content and particle size was increased. Nevertheless, these fundamental experiments with molecularly engineered model supported metal oxide

catalysts demonstrate that the catalytic activity of surface redox sites are not enhanced as the oxide support dimension is reduced to the nanoscale size. These significant findings demonstrate, *for the first time*, that catalytic redox reactions are not enhanced at the nanoscale relative to their larger conventional counterparts. The reason for this finding is that as the TiO_2 particle size becomes very small, 1–3 nm, the titania band gap slightly increases [70], which decreases electron delocalization on the titania support and to the catalytically active surface VO_4 sites that require electrons for the redox process.

4.9. Molecularly engineered model supported metal oxide catalysts

The above catalytic trend was further examined by molecularly engineering model well-defined bilayered catalysts on a catalytic relatively inert SiO_2 support [109,111,112]. The first layer of the model bilayered catalysts was synthesized by grafting two-dimensional surface oxide phases of TiO_x, ZrO_x or AlO_x onto the silica support. The second layer of surface VO_x was then grafted onto the first oxide layers. Raman characterization confirmed that crystalline phases of TiO_2, ZrO_2 or V_2O_5 were not present in any of the catalysts and that all the components were present as two-dimensional amorphous phases. Solid-state ^{27}Al NMR confirmed that the surface AlO_x species possessed AlO_4 coordination as in zeolites [113]. XANES confirmed that the surface TiO_x monolayer consisted of polymeric TiO_5 coordinated units that transformed to TiO_6 coordinated units when the surface VO_x was grafted onto the silica supported titania monolayer. The grafting of the surface VO_x species onto the surface titania monolayer is reflected in the appearance of new Raman bands associated with bridging V–O–Ti bonds at ~650 (ν_s) and ~250 (Greek letter delta) cm^{-1} and the change in the surface titania coordination upon grafting of the surface VO_x species onto the surface titania monolayer [109]. Corresponding Raman, UV–vis DRS and XANES measurements showed that the surface vanadia species were present as isolated $O{=}V(–O–S)_3$ species where S represents the underlying oxides (Fig. 4) [109,111,112].

The chemical reactivity of these bilayered supported vanadia catalysts was probed with CH_3OH oxidation and the TOF values were found to increase by a factor of ~20 in replacing some of the bridging V–O–Si bonds with bridging V–O–Zr, V–O–Ti or V–O–Al bonds. These

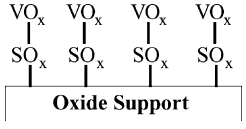

Fig. 4. Schematic of bilayered $V_2O_5/SO_x/SiO_2$ catalysts where S=Zr, Ti or Al.

fundamental results with the model well-defined bilayered catalysts clearly confirm the influence of the support cation electronegativity on the reactivity of bridging V–O–S bond.

4.10. Operando spectroscopy

Additional fundamental insights into this interesting phenomenon were obtained from *operando* IR-reactivity studies during methanol oxidation [114]. *Operando* spectroscopy was recently coined by Miguel A. Banares to describe simultaneous spectroscopic and online activity/selectivity measurements [115]. The advantage provided by *operando* spectroscopy studies is that molecular events occurring at the catalytic active sites can be directly related to the resultant catalytic activity/selectivity behavior for a given reaction. In addition, *operando* spectroscopy studies also allow for the direct determination of kinetic and thermodynamic parameters that are difficult to extract from conventional steady-state catalytic studies. For example, methanol oxidation to formaldehyde proceeds via two critical kinetic steps [116]—dissociative chemisorption of CH_3OH, which breaks the O–H bond upon adsorption, and decomposition of the resulting surface CH_3O–V intermediate to H_2CO, which breaks a C–H bond of the surface methoxy intermediate, as shown:

$$CH_3OH + V{-}O{-}S \leftrightarrow CH_3O{-}V + HO{-}S K_{ads} \quad (1)$$

$$CH_3O{-}V \rightarrow H_2CO + H{-}V k_{rds} \quad (2)$$

The *operando* IR-reactivity studies allowed for the independent quantitative determination of the adsorption equilibrium constant, K_{ads}, and the kinetic rate constant for the rate-determining-step, k_{rds}, for the surface VO_4 species on different oxide supports [114]. It was found that the thermodynamic equilibrium adsorption constant, K_{ads}, was relatively invariant as the oxide support electronegativity was changed. The kinetic rate constant, k_{rds}, however, varied significantly as the oxide support electronegativity was changed. Thus, it appears that the dramatic variation in the TOF for methanol oxidation over different supported vanadia catalysts is primarily related to changes in the kinetic k_{rds} rate constant and not changes in the thermodynamic K_{ads} equilibrium adsorption constant.

4.11. Catalytic promoters

Secondary metal oxides are many times added to supported metal oxide catalysts to further enhance the performance, activity or selectivity, of the catalytic active sites. For example, supported V_2O_5/TiO_2 SCR catalysts for NO_x reduction with NH_3 to innocuous N_2 and H_2O are typically promoted with WO_3 [94,117,118]. Raman and IR studies showed that both the vanadia and tungsten oxide components are present as surface VO_x and WO_x species on the TiO_2 support below monolayer surface coverage [119]. Methanol oxidation over the unpromoted and tungsten oxide

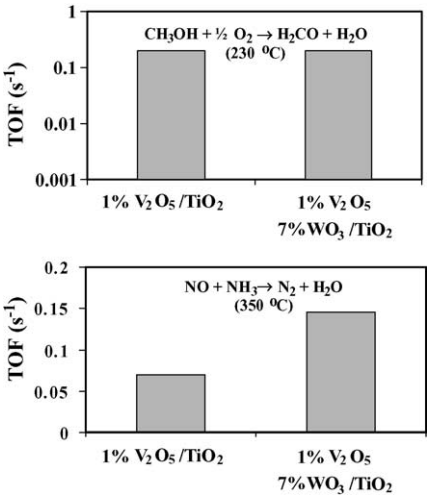

Fig. 5. The addition of acidic surface WO_x species to supported V_2O_5/TiO_2 promotes the SCR reaction, but not the redox CH_3OH oxidation reaction.

promoted V_2O_5/TiO_2 catalysts revealed that the redox TOF for the surface vanadia species is not affected by the presence of the acidic surface WO_x species (as shown in Fig. 5). The NO and NH_3 SCR reaction, however, is significantly enhanced in the presence of the acidic surface WO_x species as shown. The different response of the methanol oxidation redox reaction and the SCR reaction is related to the different surface chemical requirements of each reaction. CH_3OH oxidation to H_2CO requires only one surface redox sites while two sites are required for the adsorption of NH_3 and NO in the bimolecular SCR reaction: a surface acid site to adsorb the basic ammonia and to reduce an adjacent redox site to generate the vacancy required for the adsorption of NO since NO will not chemisorb on a fully oxidized redox site. Consequently, the presence of an acidic surface WO_x site does not affect the unimolecular CH_3OH oxidation redox reaction and does promote the bimolecular NO and NH_3 SCR reaction. Additional studies with molecularly designed model catalysts revealed that surface Bronsted acid sites are more effective promoters for the SCR reaction than surface Lewis acid sites, which also promote the SCR reaction [94,117,120]. The unimolecular SO_2 oxidation to SO_3 was also found to behave similarly to the methanol redox oxidation reaction over the same catalysts [90]. These fundamental studies revealed that (1) the surface VO_4 species supported on TiO_2 possess the same redox surface chemistry in the presence and absence of secondary acidic surface metal oxide promoters, and (2) the secondary surface metal oxide additive only becomes a promoter depending on the special chemical requirements of a given catalytic reaction. In addition, these fundamental studies also demonstrate the enormous potential of molecularly engineered supported metal oxide catalyst systems to determine, on a molecular level, the nature of the catalytic active sites for specific catalytic reactions over mixed metal oxide catalysts.

4.12. Catalytic poisons

In industrial environments, metal oxide catalytic materials are exposed to impurities that may adversely impact their catalytic performance. A typical catalyst poison for certain oxidation catalytic reactions (e.g., CH_3OH oxidation to H_2CO and SCR of NO with NH_3) is potassium oxide. Characterization studies have shown that potassium oxide directly interacts with the surface vanadia species present in supported vanadia catalysts by altering the bond lengths of the surface VO_4 species [89,121,122]. The direct interaction of the basic surface KO_x species with the surface VO_4 species results in more stable and less reducible oxygen species [89,122]. Consequently, the TOF values for all redox reactions over mixed metal oxide catalysts become significantly diminished in the presence of basic potassium oxide. For some catalytic redox reactions over mixed metal oxides, however, the basic surface KO_x species may also titrate the strong acid sites that are responsible for undesirable side reactions. Thus, similar to the addition of acidic surface metal oxides, basic surface metal oxide additives can be viewed as either promoters or poisons for a specific mixed metal oxide catalytic system depending on the special chemical requirements of a given catalytic reaction.

4.13. Spontaneous dispersion of metal oxides

It was demonstrated in the early 1980s that one crystalline metal oxide component may thermally spread as a surface MO_x species over a secondary metal oxide substrate above the Tammann temperature ($T_{TAM} = \sim\frac{1}{2}T_{MP}$ where T_{MP} is the metal oxide melting point) of the spreading metal oxide component [123–126]. This was nicely illustrated by Knozinger and co-workers with in situ Raman experiments following the *thermal* spreading of MoO_x onto different oxide supports [127]. The driving force for this surface wetting of metal oxides is the lower surface free energy of the final supported metal oxide system. The hydroxylated oxide support surface possesses a much higher surface free energy than the terminal M=O bonds formed in the surface metal oxide monolayer. The kinetics of this spreading, however, is controlled by the mobility or surface diffusion of the spreading metal oxide component [125]. It was subsequently discovered that metal oxides can also become dispersed onto oxide supports at temperatures much lower than even the Tammann temperature by interaction with reactive molecules that may be present under reaction conditions, and this has been referred to as *reaction induced dispersion* [128]. The metal oxides that have relatively low Tammann temperatures and, consequently, disperse at typical catalyst synthesis and reaction temperatures, ~100–600 °C, follow this trend with increasing T_{TAM} temperature: $CrO_3 < Re_2O_7 < V_2O_5 < MoO_3 < WO_3$. Thus, it is much easier to disperse CrO_3 than WO_3 on oxide supports and also accounts for the

presence of crystalline WO_3 nanoparticles typically present before monolayer surface coverage is reached [129]. Metal oxides, however, will not disperse on SiO_2 because of the low reactivity of its surface. Although crystalline Cr_2O_3 has a very high T_{TAM}, it is also found to readily disperse at modest temperatures because of the presence of mobile surface Cr^{+6} species on this Cr^{+3} crystalline solid [128]. Metal oxides with $T_{TAM} > 600\ ^\circ C$ can also disperse at temperatures greater than their Tammann temperature, but such elevated temperatures can also adversely affect the BET of the oxide support.

4.14. Thermal stabilization of oxide supports

Some commercial catalytic applications operate at extremely elevated temperatures of ~700–1000 °C (e.g., reforming and partial oxidation reactions to generate synthesis gas, catalytic combustion, automotive catalytic converters, etc.) where stabilization of the oxide support BET surface area is critical to the economic viability of the catalytic technology. In such circumstances, it is critical to be able to stabilize the oxide support against thermal sintering and loss of BET surface area during the lifetime of the catalyst. It has been discovered over the years that the addition of certain surface oxide species to oxide supports can dramatically retard the thermal sintering of oxide supports. Interestingly, the effective surface oxide additives tend to be those oxides that possess very high Tammann temperatures and surface oxide additives that exhibit low Tammann temperatures tend to accelerate the sintering of the oxide support [130]. These fundamental findings suggest that (1) the sintering process initiates at oxide surfaces, (2) less mobile surface oxide additives retard the sintering process by titrating the surface sites responsible for initiating sintering, and (3) more mobile surface oxide additives enhance the sintering process by accelerating the condensation of surface hydroxyls and/or reactions of oxide defects. Thus, oxide sintering is initiated by surface phenomena and, consequently, can be moderated by the addition of surface oxide additives.

4.15. Catalyst synthesis methods

A significant portion of mixed metal oxide catalysis literature has been devoted to different catalyst preparation methods and, on occasion, the proposed unique surface metal oxide species that result from specific synthesis methods. Such conclusions are, however, at odds with the discovery of spontaneous dispersion of metal oxides that reveals that the final surface metal oxide species are the thermodynamically stable state and can even be formed when beginning from physical mixtures of the crystalline metal oxide and the oxide support [123,125,126]. To further investigate this issue, a series of supported MoO_3/TiO_2 and V_2O_5/TiO_2 catalysts were prepared via all the different methods found in the literature as well as from many international laboratories [107]. The molecular structures of all the supported metal oxide catalysts were analyzed with Raman spectroscopy and found to be independent of the preparation method and even the different support types. These same findings were also made with supported surface MoO_x species on SiO_2 that were made by different synthesis methods with SiO_2 materials [131]. Differences in the surface MoO_x structure were only observed when impurities were present in the starting oxide support material [132]. Thus, the molecular structures of surface metal oxide species on oxide supports are independent of the synthesis methods, which is counter to what has been proposed in the literature for too many years.

Although the final surface metal oxide structures on SiO_2 are also independent of the particular catalyst synthesis method, aqueous versus non-aqueous and precursor salt, the partitioning between the surface MO_x species and their corresponding crystalline MO_x nanoparticles is significantly affected by the specific preparation methods [80,86,110–112,133,134]. This difference is related to the number and reactivity of the surface hydroxyls on the SiO_2 support as well as the low pH at point of zero charge of the SiO_2 support in aqueous environments (pH ~2–3). In aqueous preparation conditions above the pH at PZC, the SiO_2 support is negatively charged and repulses the negatively charged metal oxide anions. In aqueous synthesis conditions below the pH at PZC, the SiO_2 support is positively charged and readily reacts with the metal oxide anions. The very low pH requirements to disperse surface metal oxides on SiO_2 is responsible for the different partitioning between surface MO_x species and crystalline MO_x nanoparticles on SiO_2 supports typically observed in the catalysis literature.

4.16. Summary

The fundamental spectroscopic studies over the past three decades with supported metal oxide catalysts have allowed for the detection and determination of the molecular structures of surface metal oxide catalytic active sites as well as the influence of different environments on their structures. Corresponding catalytic investigations have begun to establish molecular structure-activity/selectivity relationships for many different catalytic reactions over supported mixed metal oxides. These significant advances have been accelerated by the ability to molecular engineer model well-defined supported metal oxide catalytic materials that have allowed systematic variation of the various functionalities in supported metal oxide catalytic materials.

5. Molecular sieves

As various transition metal oxide-containing molecular sieve materials began to be synthesized in the late 1980s and 1990s, it became of interest to compare their molecular structures and catalytic properties with their corresponding

Table 1
Comparison of catalytic performance of crystalline V-silicalite and amorphous 1% V_2O_5/SiO_2 during methanol oxidation at 380 °C

Catalyst	TOF (10^{-3} s^{-1}) T = 380 °C	Selectivity (%)		
		HCHO	$HCOOCH_3$	CO_x
1% V_2O_5/SiO_2	43	84.6	2.5	12.9
V-silicalite	53	87.0	0.0	13.0

supported transition metal oxides on amorphous SiO_2 catalysts. Transition metal oxide silicate molecular sieves typically possess low levels of isolated transition metal oxide in silicate structures [8]. Almost the same isolated structures are found to also be present for the supported transition metal oxides on amorphous SiO_2 catalysts [40,135,136]. Furthermore, when chemically probed for CH_3OH oxidation to H_2CO, the crystalline and amorphous analogs yield essentially the same TOF and selectivity values. The results for supported 1% V_2O_5/SiO_2 and V-silicalite are shown in Table 1:

The methanol oxidation TOF values between both types of catalysts are essentially indistinguishable within experimental error as are the H_2CO and CO_x selectivity values. These findings further suggest that the local bridging V–O–Si bond controls the catalytic activity and selectivity of the amorphous and crystalline V_2O_5–SiO_2 systems, and not the long range order of the silica matrix. This is analogous to the supported V_2O_5/TiO_2 catalytic system with different bulk titania phases discussed above. In addition, the model supported surface metal oxides on amorphous silica catalysts allow quantitative prediction of the catalytic surface chemistry for transition metal oxides in siliceous molecular sieves (silicalites, MCM-41, MCM-48, SBA, etc.) for such gas phase reactions.

5.1. Summary

The isolated transition metal oxides present in siliceous crystalline molecular sieves and on the surface of amorphous SiO_2 possess similar molecular structures and catalytic surface chemistry for vapor phase reactions. Consequently, it is now possible to predict the vapor phase catalytic activity, at least for oxidation reactions, for crystalline transition metal oxide silicate materials even prior to the successful synthesis of such catalytic materials.

6. Bulk mixed metal oxides

Bulk mixed metal oxide catalytic materials consist of large crystalline phases possessing low surface area (typically ~1–10 m^2 g^{-1}). The nature of the catalytic active sites present on the surfaces of bulk mixed metal oxide catalysts employed for selective oxidation reactions has eluded catalyst researchers over the years [6,137]. This situation is a consequence of the bulk spectroscopic techniques (XRD, Raman, IR, HR-TEM, solid-state NMR and XAS) usually used to characterize the bulk crystalline structures and the low dispersion state of mixed metal oxide catalytic materials. The bulk nature of these characterization techniques generally allows the signals from the bulk lattice to dominate the resulting spectra because of the significantly higher number of atoms in the bulk lattice than on the surface. In a few cases of mixed metal oxide catalytic materials, however, surface information has also recently been reported in the catalysis literature.

Guliants et al. obtained HR-TEM images of the layered vanadyl pyrophosphate, $(VO_2)_2P_2O_7$, catalyst and observed that the layered structure terminates with an amorphous layer rather than the crystalline lattice [57]. Consistent with this early conclusion, are the recent soft EXAFS studies by Schlogel et al. that the surface oxidation states and surface composition are different than that of the bulk lattice and are a strong function of environmental conditions [29,30]. In another recent investigation, Schlogl et al. also reported HR-TEM images of bulk mixed Mo–V–Te–Nb–O oxides showing the presence of crystalline nanoparticles at the surface of this mixed metal oxide catalyst [58]. In situ Raman measurements of bulk mixed V–Nb–O and Mo–Nb–O oxides were able to detect the surface MO_x species present in such mixed metal oxide catalytic materials [93].

The in situ Raman spectra for the bulk mixed V–Nb–O oxide formed by coprecipitation is shown in Fig. 6 as a function of vanadium oxide content. In the absence of vanadia, the Raman spectrum is dominated by a Raman band at ~700 cm^{-1} originating from the bulk Nb–O vibration of

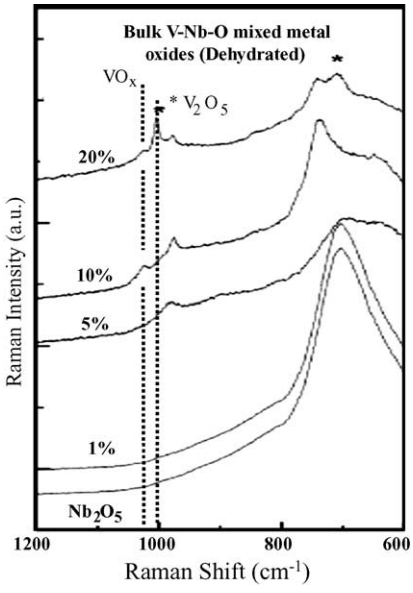

Fig. 6. Raman spectra of dehydrated coprecipitated bulk mixed V–Nb–O oxides as a function of V_2O_5 content: (a) band slightly above 1000 cm^{-1} arises from surface VO_x species, (b) band slightly below 1000 cm^{-1} originates from bulk VO_x in the mixed V–Nb–O oxide bulk lattice, (c) bands at ~1000 and 700 cm^{-1} characteristic of crystalline V_2O_5 nanoparticles, and (d) bands ~700 cm^{-1} come from bulk Nb–O vibrations.

the Nb_2O_5 [61]. As the vanadia content is increased, this Raman band shifts towards ~740 cm^{-1} because of the distortion of the bulk lattice by the incorporation of vanadia into the bulk lattice and several new vanadia bands appear in the 1000 cm^{-1} region. The initial vanadia Raman band below 1000 cm^{-1} is associated with a bulk vanadia species since it does not change its band position upon hydration and dehydration. The vanadia band above 1000 cm^{-1}, however, does change its position upon hydration and dehydration indicating that it is associated with a surface species. The Raman band position of the dehydrated surface VO_x species for the mixed V–Nb–O oxide is similar to that previously found for the surface VO_4 species present for dehydrated supported vanadium oxide catalysts. This suggests similar surface VO_4 structures for catalytic sites in both supported vanadia catalysts and mixed metal oxide catalytic materials. At the highest vanadia content, crystalline V_2O_5 bands are also present in the Raman spectrum, labeled with an asterisk, indicating that all the bulk and surface sites capable of interacting with vanadia are saturated. Essentially similar results were found for the mixed Mo–Nb–O oxide system. This series of Raman characterization studies reveals that (1) secondary cations tend to be initially incorporated into the bulk lattice of the host oxide, (2) when the bulk lattice sites are saturated, the secondary cations become concentrated at the surface of the mixed metal oxide, and (3) crystalline V_2O_5 nanoparticles form when all the surface sites are saturated. The success of Raman spectroscopy in detecting the surface VO_x species is a consequence of the absence of strong Raman bands from the bulk lattice of the V–Nb–O and Mo–Nb–O oxide phases. Corresponding propane ODH catalytic studies clearly demonstrated that the surface VO_4 species, and not the bulk vanadia or crystalline V_2O_5 components are the catalytic active sites for the mixed V–Nb–O oxide catalyst system (similarly for the mixed Mo–Nb–O catalyst system).

The presence of the same elements in the bulk crystalline lattice and on the surface and in the bulk lattice does not allow many surface analytical techniques to discriminate between the bulk and surface cations of mixed metal oxide catalytic materials because of the ~3–5 nm sampling depth of typical electron spectroscopic techniques (e.g., XPS, AES, etc.). Low energy ion scattering spectroscopy (LEISS), however, employs noble gas ions, such as He^+, that only scatter from the outer surface and can provide elemental information about the outermost surface layer. This has been employed by Gruenert et al. to characterize the surfaces of a series of bulk mixed metal vanadates [138]. It was surprisingly discovered that all the examined bulk mixed metal vanadates possess an amorphous surface VO_x monolayer on the crystalline lattice substrate. This conclusion was reached because the LEISS signals for the secondary metal oxide components could not be detected. The surfaces of these mixed metal vanadates were chemically probed with CH_3OH–TPSR and methanol oxidation steady-state studies. The CH_3OH–TPSR spectrum for bulk $AlVO_4$ did not exhibit the formation of DME from acidic surface Al sites and only exhibited the H_2CO product from surface redox sites of surface vanadia [139]. Furthermore, the H_2CO T_p temperature coincided with that observed for formaldehyde formation from supported V_2O_5/Al_2O_3 catalysts indicating that the surface VO_x layer present on the bulk $AlVO_4$ phase is also influenced by the underlying Al cations. These conclusions are consistent with the steady-state methanol oxidation studies over the mixed metal vanadate catalysts that demonstrated the surface chemistry of only vanadia sites [75].

The above recent findings about the surface nature of bulk mixed metal oxide catalytic materials are very exciting and creating a paradigm shift in the fundamental understanding of how such mixed metal oxides function as selective oxidation catalysts. For the past 30 years, research on bulk mixed metal oxide catalytic materials focused on the crystalline phases and their relationships to their characteristics as selective oxidation reactions [6,137]. The recent findings about the surface nature of mixed metal oxide catalysts suggest that the most important aspect of such catalytic materials was completely overlooked: the catalytic active sites present on the outermost surface layer. Only oxygen anions can be transported between the bulk lattice and the outermost surface layer, and the influence of the crystalline structure and phase on this phenomenon is not fully understood at present. Nevertheless, whether the oxygen participating comes from the bulk lattice or gas phase, it is reacting with the reactant molecule at the surface catalytic sites. Thus, much more research will be taking place in coming years on the surface nature of bulk mixed metal oxide catalytic materials and their surface chemistry characteristics.

6.1. Summary

Recent characterization studies have revealed that bulk mixed metal oxide catalytic materials contain surface metal oxide phases that can possess electronic and molecular structures that are different than in the bulk lattice. This new finding has major ramifications for the models of how bulk mixed metal oxides function as selective oxidation catalysts.

7. Conclusions

The catalysis science of mixed metal oxide catalytic materials has undergone a significant evolution, or paradigm shift, over the past three decades due to development of advanced characterization techniques that are allowing more fundamental insights to be monitored. Initially, only crystalline metal oxide phases were determined by XRD characterization and all the catalytic models were based on this bulk structural information. This situation began to change ~30 years ago as more powerful characterization

techniques became available that could provide information about amorphous metal oxide phases, as well as crystalline nanophases, under different environmental conditions. The first major breakthrough was the discovery and subsequent confirmation that amorphous surface species exist for supported metal oxide catalysts, which opened up an entirely new area of catalysis research. More recent studies demonstrated that the same metal oxide catalytic active sites are present for crystalline siliceous molecular sieves and their corresponding amorphous SiO_2-supported metal oxide analogs. Furthermore, the same catalytic properties are exhibited by both the crystalline molecular sieves and the amorphous SiO_2-based catalysts revealing the importance of local environment over long range order in mixed metal oxides. Most recently, the discovery of the presence of amorphous surface species on the surface of bulk mixed metal oxide materials is having a significant impact on how catalysis researchers think about such catalytic materials. Thus, the presence of amorphous surface species and phases in mixed metal oxide catalytic materials and their electronic/molecular structures–catalytic activity/selectivity relationships are now at the forefront of the catalysis science of mixed metal oxide materials. This new research paradigm will have significant impact on the catalysis models of mixed metal oxides in the coming years. In summary, the more complex catalysis science of mixed metal oxide catalysts is finally catching up to the catalysis science of metal catalysts.

Acknowledgments

This article is dedicated to my numerous collaborators and graduate students at Lehigh University who have contributed to the advances in the catalysis science of mixed metal oxide catalytic materials (their names are listed in the joint publications in the reference section). Without their collective contributions, all the current insights about mixed metal oxide catalytic materials would not be available. The financial support of NSF-CTS-0213377 and DOE-Basic Energy Sciences (DE-FG02-93ER14350) for research on mixed metal oxide catalysis over the years is gratefully acknowledged. The Ministerio de Educacion y Ciencia visiting scientist/sabbatical grant SAB-2003-0212 is much appreciated and the Instituto de Catalisis and Petroleoquimica, CSIC, is also acknowledged for its hospitality during the writing of this article.

References

[1] M. Boudart, G. Djéga-Mariadassou, Kinetics of Heterogeneous Catalytic Reactions, Princeton University Press, Lawrenceville, New Jersey, 1984.
[2] G.A. Somorjai, Chemistry in Two-Dimensions: Surfaces, Cornell University Press, Ithaca, New York, 1981.
[3] G.A. Somorjai, Introduction to Surface Chemistry and Catalysis, Wiley, New York, 1994.
[4] J. Schwank, Bulk metals and alloys, in: I.E. Wachs (Ed.), Characterization of Catalytic Materials, Butterworth-Heinemann, Boston, Massachusetts, 1992, pp. 1–16.
[5] G. Metzner, Supported metal catalysts, in: I.E. Wachs (Ed.), Characterization of Catalytic Materials, Butterworth-Heinemann, Boston, Massachusetts, 1992, pp. 17–45.
[6] J.F. Brazdil, Bulk metal oxides, in: I.E. Wachs (Ed.), Characterization of Catalytic Materials, Butterworth-Heinemann, Boston, Massachusetts, 1992, pp. 47–68.
[7] I.E. Wachs, K. Segawa, Supported metal oxides, in: I.E. Wachs (Ed.), Characterization of Catalytic Materials, Butterworth-Heinemann, Boston, Massachusetts, 1992, pp. 69–88.
[8] M.E. Davis, J.B. Higgins, Zeolites and molecular sieves, in: I.E. Wachs (Ed.), Characterization of Catalytic Materials, Butterworth-Heinemann, Boston, Massachusetts, 1992, pp. 129–148.
[9] T. Yamase, M.T. Pope, D.J. Lockwood (Eds.), Polyoxometalate Chemistry for Nano-Composite Design, Kluwer Academic/Plenum Publishers, 2002.
[10] L.E. Briand, G.T. Baronetti, H.J. Thomas, Appl. Catal. A: General 256 (2003) 37.
[11] J.E. Mapes, R.P. Eischens, J. Phys. Chem. 58 (1954) 1059.
[12] J.H. Lunsford, Catal. Rev. 8 (1973) 265.
[13] T.A. Carlson (Ed.), X-ray Photoelectron Spectroscopy, Dowden, Hutchinson & Ross, Inc., Stroudsburg, 1978.
[14] C.D. Wagner, W.M. Riggs, L.E. Davis, J.F. Moulder, G.E. Muilenberg, Handbook of X-ray Photoelectron Spectroscopy: A Reference Book of Standard Spectra for Identification and Interpretation of XPS Data, Perkin-Elmer Corporation, 1979.
[15] S.S. Chan, I.E. Wachs, L.L. Murrell, L. Wang, W.K. Hall, J. Phys. Chem. 88 (1984) 5831.
[16] F.R. Brown, L.E. Makovsky, K.H. Rhee, Appl. Spectrosc. 31 (1977) 563;
F.R. Brown, L.E. Makovsky, K.H. Rhee, J. Catal. 50 (1977) 162;
F.R. Brown, L.E. Makovsky, K.H. Rhee, J. Catal. 50 (1977) 385.
[17] R. Thomas, J.A. Moulijn, F.P.J.M. Kerkhof, Recueil des Travaux Chimiques des Pays-Bas 96 (1977) 134.
[18] F. Roozeboom, M.C. Mittelmeijer-Hazeleger, J.A. Moulijn, J. Medema, V.H.J. De Beer, P.J. Gellings, J. Phys. Chem. 84 (1980) 2783.
[19] F. Roozeboom, J. Medema, P.J. Gellings, Zeitschrift fuer Physikalische Chemie 111 (1978) 215.
[20] F.P.J.M. Kerkhof, J.A. Moulijn, R. Thomas, J. Catal. 56 (1979) 279.
[21] C.P. Cheng, J.D. Ludowise, G.L. Schrader, Appl. Spectrosc. 34 (1980) 146.
[22] L. Wang, W.K. Hall, J. Catal. 82 (1983) 177.
[23] J.M. Stencel, L.E. Makovsky, T.A. Sarkus, J. De Vries, R. Thomas, J.A. Moulijn, J. Catal. 90 (1984) 314.
[24] J.M. Stencel, L.E. Makovsky, J.R. Diehl, T.A. Sarkus, J. Raman Spectrosc. 15 (1984) 282.
[25] E.A. Stern, Historical developments of EXAFS, in: R.K. Teo, D.C. Joy (Eds.), EXAFS Spectroscopy: Techniques and Applications, Plenum Press, New York, 1981, pp. 1–4.
[26] D.E. Sayers, E.A. Stern, F.W. Lytle, Phys. Rev. Lett. 27 (1971) 1204.
[27] F.W. Lytle, D.E. Sayers, E.A. Stern, Phys. Rev. B11 (1975) 4825.
[28] A. Knop-Gericke, M. Haveker, T. Schedel, R. Schlogl, Top. Catal. 15 (2001) 27.
[29] H. Bluhm, D.F. Ogletree, C.H. Fadley, Z. Haussain, M. Salmeron, Phys. Condes. Matter 14 (2002) 227.
[30] A. Knop-Gericke, F.M.F. de Groot, J.A. van Bokhoven, T. Ressler, Soft X-ray absorption methods, in: B.M. Weckhuysen (Ed.), In Situ Spectrospcoy of Catalysts, American Scientific Publishers, California, 2004, pp. 145–160.
[31] M. Hunger, J. Weitkamp, Nuclear magnetic resonance, in: B.M. Weckhuysen (Ed.), In Situ Spectroscopy of Catalysts, American Scientific Publishers, California, 2004.
[32] D.M. Anufriev, K.G. Ione, O.B. Lapina, V.M. Mastikhin, Doklady Akademii Nauk SSSR 243 (4) (1978) 945.

[33] V.M. Mastikhin, O.B. Lapina, V.F. Lyakhova, Reaction Kinet. Catal. Lett. 14 (1980) 323.
[34] V.M. Mastikhin, O.B. Lapina, V.F. Lyakhova, Reaction Kinet. Catal. Lett. 14 (1980) 317.
[35] H. Eckert, I.E. Wachs, In microstructure and properties of catalysts, Mater. Res. Soc. Symp. Proc. 111 (1988) 459.
[36] H. Eckert, I.E. Wachs, J. Phys. Chem. 93 (1989) 6796.
[37] E.C. Decanio, J.C. Edwards, T.R. Scalzo, D.A. Storm, J.W. Bruno, J. Catal. 132 (1991) 498.
[38] J.C. Edwards, R.D. Adams, P.D. Ellis, J. Am. Chem. Soc. 112 (1990) 8349.
[39] M. Niwa, N. Katada, Y. Murakami, J. Catal. 134 (1992) 340.
[40] C.B. Wang, G. Deo, I.E. Wachs, J. Catal. 178 (1998) 640.
[41] H. Eckert, in: A.T. Bell, A. Pines (Eds.), NMR Techniques in Catalysis, Marcel Dekker, New York, 1994.
[42] M.E. Lashier, G.L. Schrader, B.C. Gerstein, Appl. Catal. 73 (1991) 83.
[43] K. Klier, J. Opt. Soc. 62 (1972) 882.
[44] R. Kellerman, Diffuse reflectance and photoacoustic spectroscopie, in: W.N. Delgass, G.L. Haller, R. Kellerman, J.H. Lunsford (Eds.), Spectroscopy in Heterogeneous Catalysis, Academic Press, New York, 1979, p. 86.
[45] K. Klier, in: A.T. Bell, M.L. Hair (Eds.), Vibrational Spectroscopies for Adsorbed Species, 137, ACS Symp. Ser, 1980, p. 141.
[46] F. Vergand, D. Fargues, D. Oliver, L. Bonneviot, M. Che, J. Phys. Chem. 87 (1983) 2373.
[47] R.A. Schoonheydt, in: F. Delannay (Ed.), Characterization of Catalysts, Marcel Dekker, New York, 1984, p. 125.
[48] M. Fournier, C. Louis, M. Che, P. Chaquin, D. Masure, J. Catal. 119 (1989) 400.
[49] R.S. Weber, J. Catal. 151 (1995) 470.
[50] B.M. Weckhuysen, R.A. Schoonheydt, J.-M. Jehng, I.E. Wachs, S.J. Cho, R. Ryoo, S. Kijlstra, E. Poels, J. Chem. Soc., Faraday Trans. 91 (1995) 3245.
[51] B.J. Tatarchuk, J.J. Chludzinski, R.D. Sherwood, J.A. Dumesic, R.T.K. Baker, J. Catal. 70 (1981) 433.
[52] P.L. Gai, Top. Catal. 21 (2002) 161.
[53] P.L. Hansen, J.B. Wagner, S. Helveg, J.R. Rostrup-Nielsen, B.S. Clausen, H. Topsoe, Science 295 (2002) 2053.
[54] T.W. Hansen, J.B. Wagner, B. Jakob, P.L. Hansen, S. Dahl, H. Topsoe, C.J.H. Jacobsen, Science 294 (2001) 1508.
[55] S. Helveg, J.V. Lauritsen, E. Laegsgaard, I. Stensgaard, J.K. Norskov, B.S. Clausen, H. Topsoe, F. Besenbacher, Phys. Rev. Lett. 84 (2000) 951.
[56] S. Bernal, R.T. Baker, A. Burrows, J.J. Calvino, C.J. Kiely, C. Lopez-Cartes, J.A. Perez-Omil, J.M. Rodriguez-Izquierdo, Surf. Interf. Anal. 29 (2000) 411.
[57] V.V. Guliants, J.B. Benziger, S. Sundaresan, N. Yao, I.E. Wachs, Catal. Lett. 32 (1995) 379.
[58] R. Schlogl, D. Teschner, A. Knop-Gericke, M. Haevecker, E. Kleimenov, D. Su, The function of VxOy species in selective oxidation: An in-situ high pressure XPS studies (abstracts of papers), in: 228th ACS National Meeting, Philadelphia, PA, United States, August 22–26, 2004, COLL-194.
[59] J.M. Tatibouet, Appl. Catal. A: 148 (1997) 213.
[60] A.F. Wells, Structural Inorganic Chemistry, Oxford University Press, New York, 1984.
[61] J.-M. Jehng, I.E. Wachs, Chem. Mat. 3 (1991) 100.
[62] G. Busca, G. Ramis, V. Lorenzelli, J. Mol. Catal. 50 (1989) 231.
[63] A. Davydov, in: N.T. Sheppard (Ed.), Molecular Spectroscopy of Oxide Catalyst Surfaces, Wiley, Hoboken, 2003.
[64] J. Haber, Crystallography of catalyst types, in: M. Boudart, J.R. Anderson (Eds.), Catalysis, 2, Springer, Berlin, 1984, p. 13.
[65] H.-P. Boehnm, H. Knozinger, Nature and estimation of functional groups on solid surfaces, in: M. Boudart, J.R. Anderson (Eds.), Catalysis, 4, Springer, Berlin, 1984, p. 39.
[66] K. Tanabe, Solid Acids and Base: Their Catalytic Properties, Kodansha, Tokyo, 1970.
[67] V.M. Mastikhin, A.V. Nosov, V.V. Terskikh, K.I. Zamaraev, I.E. Wachs, J. Phys. Chem. 98 (1994) 13621.
[68] C. Setzer, G. van Essche, N. Pryor, Silica, in: F. Schuth, K.S.W. Sing, J. Weitkamp (Eds.), Handbook of Porous Solids, Wiley-VCH, Berlin, 2004, p. 1543.
[69] P. Euzen, P. Raybaud, X. Krokidis, H. Toulhoat, J.-L. Le Loarer, J.-P. Jolivet, C. Froidefond, Alumina, in: F. Schuth, K.S.W. Sing, J. Weitkamp (Eds.), Handbook of Porous Solids, Wiley-VCH, Berlin, 2004, p. 1591.
[70] M. Fernandez-Garcia, A. Martinez-Arias, J.C. Hanson, J.A. Rodriguez, Chem. Rev. 104 (2004) 4063.
[71] J. Datka, A.M. Turek, J.-M. Jehng, I.E. Wachs, J. Catal. 135 (1992) 186.
[72] G. Busca, J. Mol. Catal. 50 (1989) 241.
[73] W.E. Farneth, F. Ohuchi, R.H. Staley, U. Chowdhry, A.W. Sleight, J. Phys. Chem. 89 (1985) 2493.
[74] M. Badlani, I.E. Wachs, Catal. Lett. 75 (2001) 137.
[75] L.E. Briand, J.-M. Jehng, L. Cornaglia, A.M. Hirt, I.E. Wachs, Catal. Today 78 (2003) 257.
[76] I.E. Wachs, Y. Chen, J.-M. Jehng, L.E. Briand, T. Tanaka, Catal. Today 78 (2003) 13.
[77] J. Haber, M. Witko, R. Tokarz, Appl. Catal. A: General 157 (1997) 3.
[78] A.M. Turek, I.E. Wachs, E. DeCanio, J. Phys. Chem 96 (1992) 5000.
[79] M.A. Vuurman, D.J. Stufkens, A. Oskam, I.E. Wachs, J. Chem. Soc., Faraday Trans. 17 (92) (1996) 3259;
M.A. Vuurman, I.E. Wachs, J. Mol. Catal. 77 (1992) 29.
[80] M. de Boer, A.J. van Dillen, D.C. Koningsberger, J. Geus, M.A. Vuurman, I.E. Wachs, Catal. Lett. 11 (1991) 227.
[81] F. Kapteijn, A.D. van Langeveld, J.A. Moulijn, A. Andreini, M.A. Vuurman, A.M. Turek, J.-M. Jehng, I.E. Wachs, J. Catal. 150 (1994) 94.
[82] C.L. Thomas, Catalytic Processes and Proven Catalysts, Academic Press, New York, 1970.
[83] T. Tanaka, H. Yamashita, R. Tsuchitani, T. Funabiki, S. Yoshida, J. Chem. Soc., Faraday Trans. 1 (84) (1988) 2987.
[84] C. Cristiani, P. Forzatti, G. Busca, J. Catal. 116 (1989) 588.
[85] I.E. Wachs, F.D. Hardcastle, Proc. Ninth Int. Congr. Catal. 3 (1988) 1449.
[86] X. Gao, S.R. Bare, B.M. Weckhuysen, I.E. Wachs, J. Phys. Chem. B 102 (1998) 10842.
[87] H. Tian, I.E. Wachs, in press.
[88] G. Deo, I.E. Wachs, J. Catal. 129 (1991) 307.
[89] G. Deo, I.E. Wachs, J. Catal. 146 (1994) 323.
[90] J.P. Dunn, H.G. Stenger Jr., I.E. Wachs, J. Catal. 181 (1999) 301.
[91] X. Gao, M.A. Banares, I.E. Wachs, J. Catal. 188 (1999) 325.
[92] X. Gao, J.-M. Jehng, I.E. Wachs, J. Catal. 209 (2002) 43.
[93] Z. Zhao, X. Gao, I.E. Wachs, J. Phys. Chem. B 107 (2003) 6333.
[94] I.E. Wachs, G. Deo, B.M. Weckhuysen, A. Andreini, M.A. Vuurman, M. de Boer, M.D. Amiridis, J. Catal. 161 (1996) 211.
[95] I.E. Wachs, J.-M. Jehng, G. Deo, B.M. Weckhuysen, V.V. Guliants, J.G. Benziger, S. Sundaresan, J. Catal. 170 (1997) 75.
[96] C. Zhao, I.E. Wachs, Selective oxidation of propylene to oxygenates over supported vanadium oxide catalysts (abstracts of papers), in: 228th ACS National Meeting, Philadelphia, PA, United States, August 22–26, 2004, COLL-224.
[97] L.J. Burcham, G. Deo, X. Gao, I.E. Wachs, Top. Catal. 11/12 (2000) 85.
[98] T. Feng, J.M. Vohs, J. Catal. 208 (2002) 301.
[99] T. Feng, J.M. Vohs, J. Catal. 221 (2004) 619.
[100] G.S. Wong, M.R. Concepcion, J.M. Vohs, J. Phys. Chem. B 106 (2002) 6451.
[101] G.S. Wong, D.D. Kragten, J.M. Vohs, J. Phys. Chem. B 105 (2001) 1366.
[102] G. Froment, K.B. Bischoff, Chemical Reactor Analysis and Design, Wiley, New York, 1979.
[103] S. Choi, I.E. Wachs, Selective oxidesulfurization of C1-organosulfur compounds over supported metal oxide catalysts (abstracts of

papers), in: 223rd ACS National Meeting, Orlando, FL, United States, April 7–11, 2002, 2002, FUEL-059.
[104] S. Choi, I.E. Wachs, in press.
[105] X. Gao, I.E. Wachs, J. Phys. Chem. B 104 (2000) 1261.
[106] I.E. Wachs, Catalysis 13 (1997) 37.
[107] G. Deo, A.M. Turek, I.E. Wachs, T. Machej, J. Haber, N. Das, H. Eckert, A.W. Hirt, Appl. Catal. A: General 91 (1992) 27;
T. Machej, J. Haber, A.M. Turek, I.E. Wachs, Appl. Catal. 70 (1991) 115.
[108] I.E. Wachs, B.M. Weckhuysen, Appl. Catal. A: General 157 (1997) 67.
[109] X. Gao, S.R. Bare, J.L.G. Fierro, I.E. Wachs, J. Phys. Chem. B 103 (1999) 618.
[110] X. Gao, S.R. Bare, J.L.G. Fierro, M.A. Banares, I.E. Wachs, J. Phys. Chem. B 102 (1998) 5653.
[111] X. Gao, J.L.G. Fierro, I.E. Wachs, Langmuir 15 (1999) 3169.
[112] X. Gao, I.E. Wachs, J. Catal. 192 (2000) 18.
[113] O.B. Lapina, E. Lee, I.E. Wachs, in press.
[114] L.J. Burcham, M. Badlani, I.E. Wachs, J. Catal. 203 (2001) 104.
[115] B.M. Weckhuysen, Chem. Commun. 2 (2002) 97.
[116] M. Boudart, AIChE J. 18 (1972) 465.
[117] M.D. Amiridis, I.E. Wachs, G. Deo, J.-M. Jehng, D.S. Kim, J. Catal. 161 (1996) 247.
[118] M.D. Amiridis, R.V. Duevel, I.E. Wachs, Appl. Catal. B: Env. 20 (1999) 111.
[119] M.A. Vuurman, I.E. Wachs, A.M. Hirt, J. Phys. Chem. 95 (1991) 9928.
[120] I.E. Wachs, G. Deo, A. Andreini, M.A. Vuurman, M. de Boer, J. Catal. 160 (1996) 322.
[121] G. Garcia Cortez, J.L.G. Fierro, M.A. Banares, Catal. Today 78 (2003) 219.
[122] X. Wang, I.E. Wachs, Catal. Today 96 (2004) 211.
[123] Y.C. Xie, Y.Q. Tang, Adv. Catal. 37 (1990) 1.
[124] J. Haber, T. Machej, T. Czeppe, Surf. Sci. 151 (1985) 301.
[125] J. Haber, T. Machej, E.M. Serwicka, I.E. Wachs, Catal. Lett. 32 (1995) 101.
[126] H. Knozinger, E. Taglauer, Catalysis 10 (1993) 1.
[127] J. Leyer, D. Mey, H. Knozinger, J. Catal. 124 (1990) 349.
[128] C.B. Wang, Y. Cai, I.E. Wachs, Langmuir 15 (1999) 1223.
[129] S.S. Chan, I.E. Wachs, L.L. Murrell, N.C. Dispenziere Jr., J. Catal. 92 (1985) 1.
[130] I.E. Wachs, J.-M. Jehng, F.D. Hardcastle, Sol. St. Ion. 32–33 (1989) 904.
[131] M.A. Banares, H. Hu, I.E. Wachs, J. Catal. 150 (1994) 407.
[132] M.A. Banares, M.D. Jones, N.D. Spencer, I.E. Wachs, J. Catal. 146 (1994) 204.
[133] C.C. Williams, J.G. Ekerdt, J.-M. Jehng, F.D. Hardcastle, A.M. Turek, I.E. Wachs, J. Phys. Chem. 95 (1991) 8781.
[134] D.S. Kim, M. Ostromecki, I.E. Wachs, J. Mol. Catal. A: Chemical 106 (1996) 93.
[135] G. Deo, A.M. Turek, I.E. Wachs, D.R.C. Huybrechts, P.A. Jacobs, Zeolites 13 (5) (1993) 365.
[136] X. Gao, M.S. Wong, J.Y. Ying, I.E. Wachs, J. Catal. 203 (2001) 18.
[137] R.K. Grasselli, J.F. Brazdil (Eds.), ACS Symposium series, vol. 279: Solid-state chemistry in catalysis. Based on a Symposium Sponsored by the Division of Petroleum Chemistry, Inc. at the 186th Meeting of the American Chemical Society, Washington, DC August 28–September 2, 1983, 1985.
[138] W. Gruenert, L. Briand, O.P. Tkachenko, N.N. Tolkatchev, I.E. Wachs, Surface composition of supported and bulk mixed metal oxide catalysts: New insight from ion scattering spectroscopic studies (abstracts of papers), in: 228th ACS National Meeting, Philadelphia, PA, United States, August 22–26, 2004, COLL-058.
[139] G. Deo, L.E. Briand, I.E. Wachs, in press.